

Supplemental materials for

Effect of atomic substitution and structure on thermal conductivity in monolayers H-MN and T-MN (M= B, Al, Ga)

Yulin Zhang¹, Siyu Gan², Jialu Li², Yi Tian¹, Xihao Chen³, Gehong Su^{4,*}, Yu Hu^{1,5,*}, and

Ning Wang^{2,*}

¹ School of New Energy Materials and Chemistry, Leshan Normal University, Leshan, Sichuan 614000, China

² School of Science, Key Laboratory of High-Performance Scientific Computation, Xihua University, Chengdu, 610039, China

³ School of Materials Science and Engineering, Chongqing University of Arts and Sciences, Chongqing, 402160, China

⁴ College of Science, Sichuan Agricultural University, Xin Kang Road, Yucheng District, Ya'an 625014, China

⁵ Leshan West Silicon Materials Photovoltaic and New Energy Industry Technology Research Institute, Leshan, Sichuan 614000, China

* Correspondence: gehongsu@sicau.edu.cn (Gehong Su); huyugucas@126.com (Yu Hu);

ningwang0213@163.com (Ning Wang)

Figure S1 shows the results of the κ_l convergence test with respect to the Q-grid and cutoff parameters. In this paper, a denser $100 \times 100 \times 1$ Q-grid mesh is used to calculate the corresponding

heat transfer performance and thermal conductivity, and the interaction cutoff value of the third-order IFC is set to the 10th nearest neighbor atom, which can achieve good convergence standards.

To investigate the impact of exchange-dependent functional selection on the thermal transport properties of H-MN and T-MN materials, we employed five different functional methods to calculate the phonon dispersion curves of eight materials, as illustrated in FIG.S2. The results show that the lattice constant of H-MN and T-MN materials are similar to each other under different functional conditions, which indicates that the effect of different functional on the lattice structure is relatively small. For example, T-AlN has the largest lattice constant using the revPBE function (6.19 Å) and the smallest lattice constant using the LDA function (6.09 Å), and the difference between the two is very small. We also observe that their maximum vibration frequencies are not significantly different. For instance, the highest vibration frequency calculated for H-BN using the sol function is 1497.91 cm^{-1} , while that calculated using PBE is 1483.85 cm^{-1} , representing a difference of only 0.94%. In addition, the phonon dispersion curves calculated by different functionals show similar characteristics, such as the same shape of phonon dispersion

curves and the high overlap of acoustic branches. This shows that different functional descriptions of phonon properties are relatively consistent. In summary, our results show that the thermal transport properties of H-MN and T-MN materials are less sensitive to the choice of exchange-correlation functional.

In order to gain a deeper understanding of the electronic properties of the 2DIII-A nitrogen, we calculated its electron band structure. The electronic band structures of H-MN and T-MN are depicted in the FIG.S3. The findings reveal that H-MN and T-MN demonstrate the characteristics of an indirect band-gap semiconductor, with calculated band-gap values ranging from 2.02 to 3.38 eV. In contrast to graphene, a well-known two-dimensional material with no band gap, the band gap features of H-MN and T-MN offer increased flexibility and controllability.

To describe the phonon anharmonicity of several materials more directly, the atomic vibration image of Γ point is shown in the supplementary file. It can be seen that the atomic vibration of the T-phase material is more intense than that of the H phase, which is mainly manifested as the relative sliding between atoms, and this phenomenon is particularly obvious in the LA phonon mode. This is because the T-phase atoms are closer to the ionic bond characteristics, and their strong long-range Coulomb

electrostatic repulsion makes the atoms easy to slide, and thus have stronger phonon anharmonicity, which is consistent with the results in ELF and Grüneisen parameters.

Fig .S4 shows the change law curve of cumulative lattice thermal conductivity and frequency. It can be seen that the cumulative lattice thermal conductivity of H-MN and T-MN increases rapidly with the increase of frequency, and no longer depends on frequency change after reaching the peak value. This indicates that the lattice thermal conductivity of these eight materials is mainly contributed by low frequency (<10 THz) phonons. This indicates that the lattice thermal conductivity of these eight materials is mainly contributed by low frequency (<10 THz) phonons.

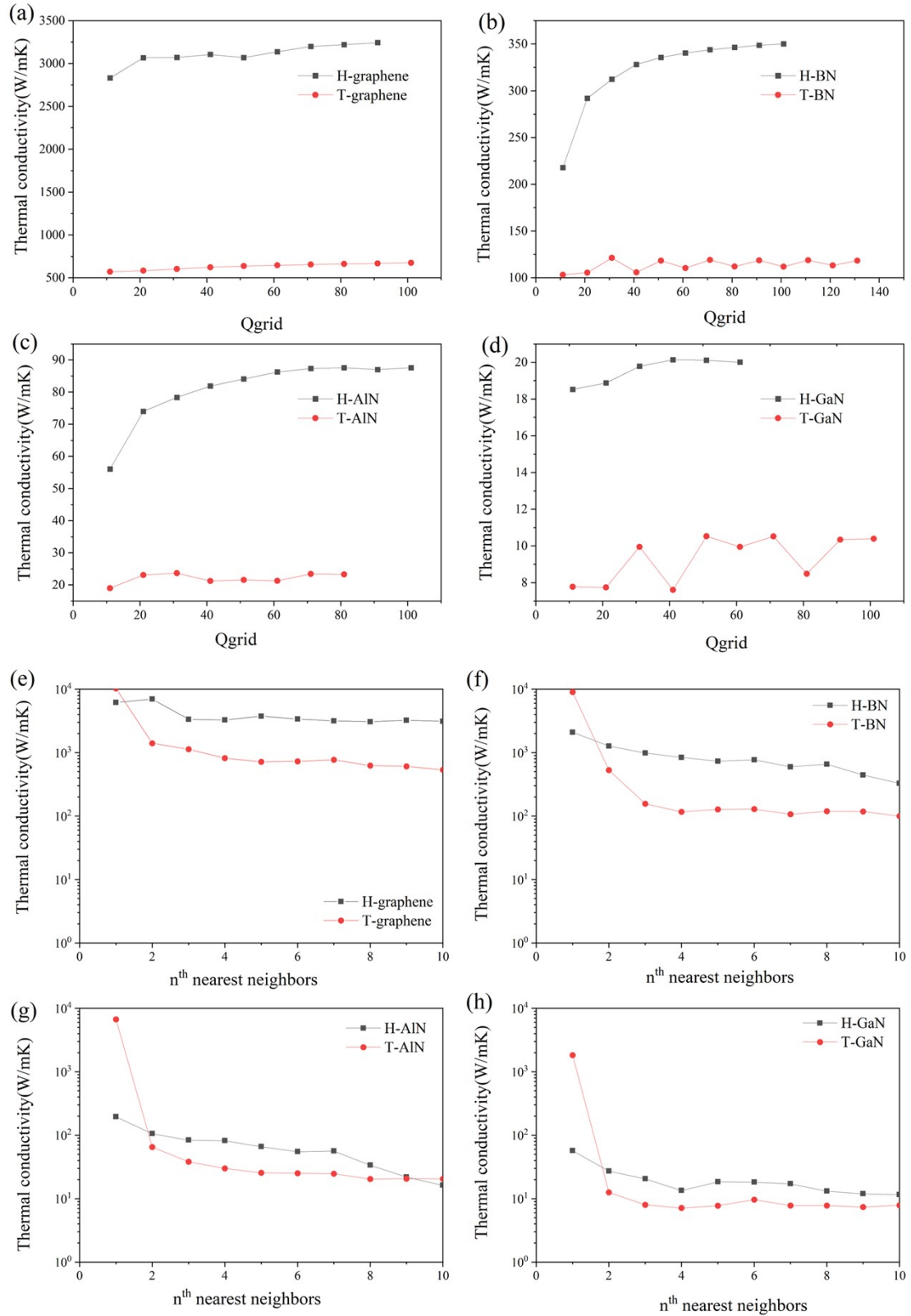


FIG.S1. Convergence test results of the thermal conductivity with respect to the nearest neighbors and Q-grid for the H-MN and T-M

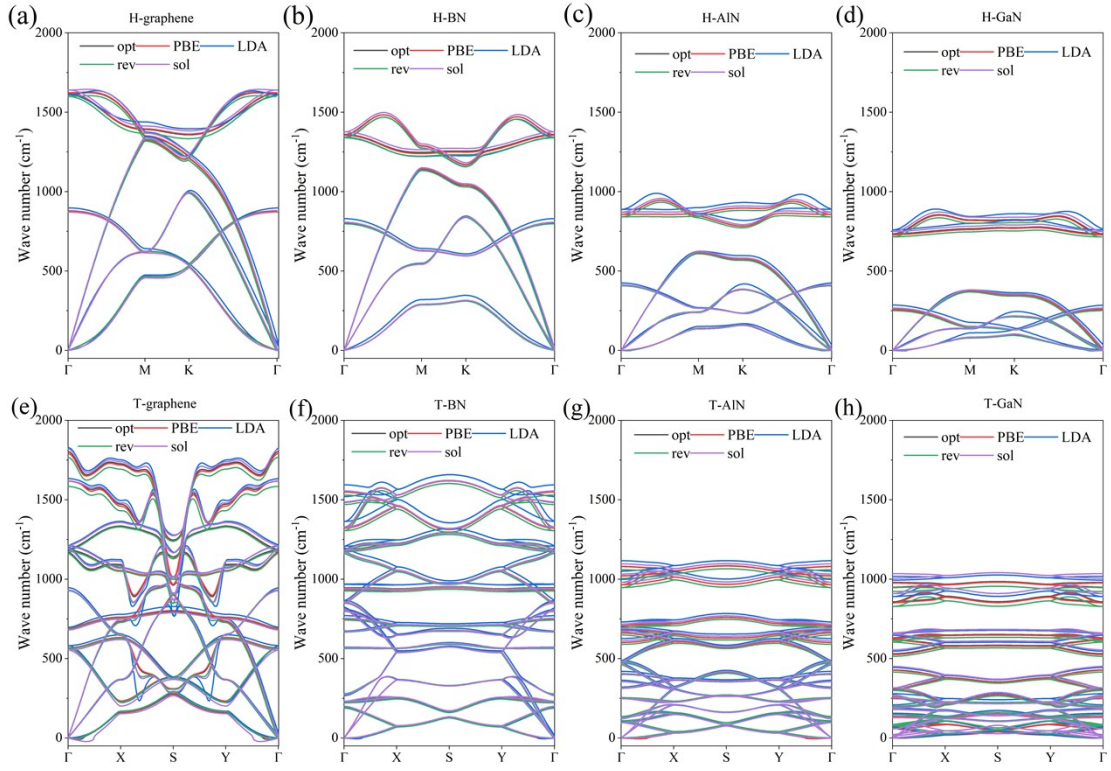


FIG.S2. Phonon dispersion of H-MN and T-MN under different functionals.

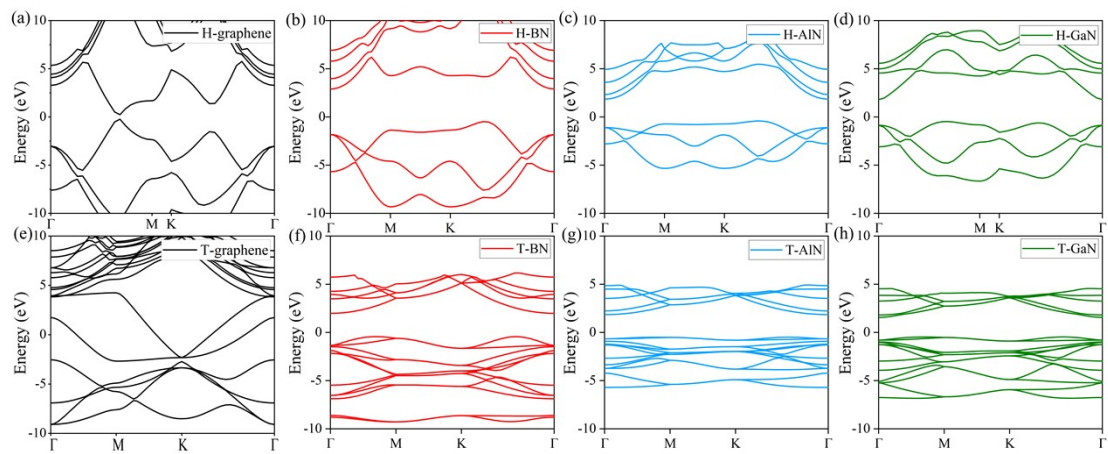


FIG.S3. Electronic band structure of H-MN and T-MN.

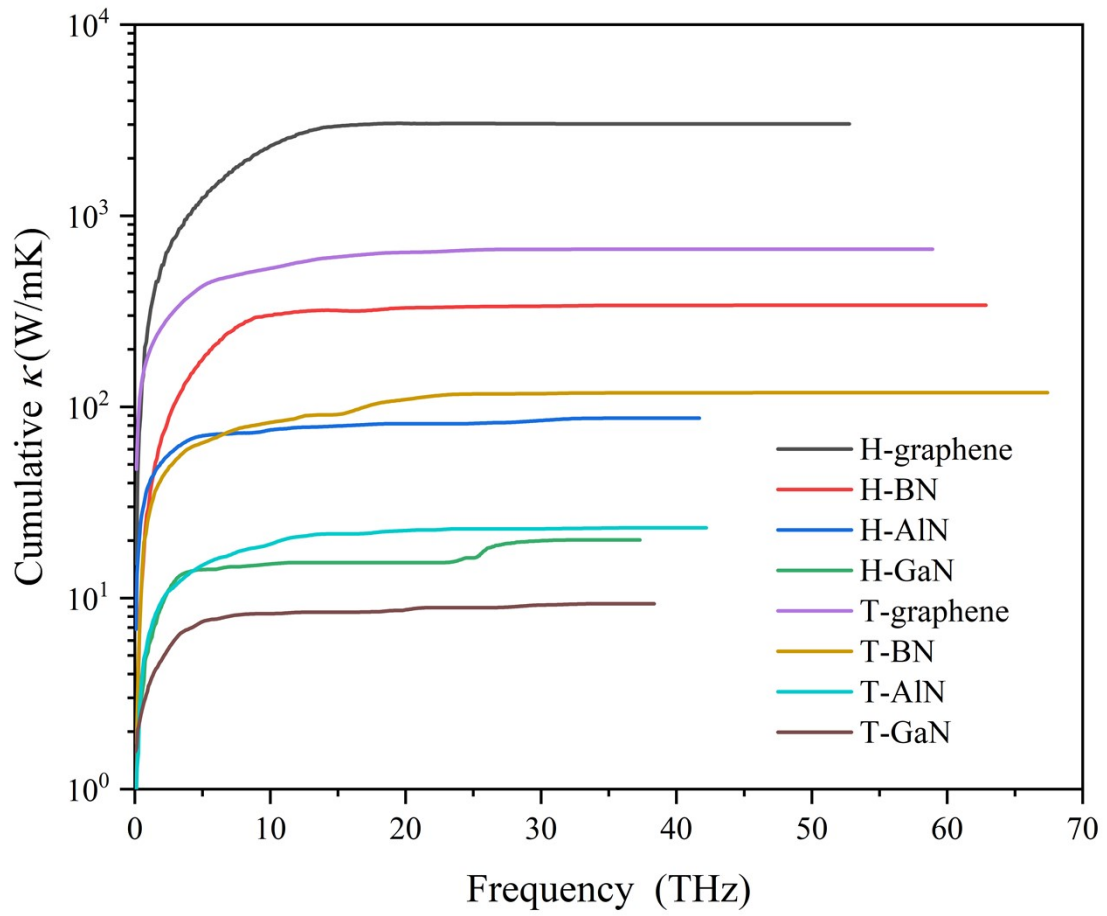


Fig .S4. Cumulative lattice thermal conductivity with frequency.